Density of states from mode expansion of the self-dynamic structure factor of a liquid metal

E. Guarini,[1] S. Bellissima,[1,2] U. Bafile,[2] E. Farhi,[3] A. De Francesco,[4] F. Formisano,[4] and F. Barocchi[1]

[1]*Dipartimento di Fisica e Astronomia, Università degli Studi di Firenze, via G. Sansone 1, I-50019 Sesto Fiorentino, Italy*

[2]*Consiglio Nazionale delle Ricerche, Istituto dei Sistemi Complessi, via Madonna del Piano 10, I-50019 Sesto Fiorentino, Italy*

[3]*Institut Laue-Langevin, 71 avenue des Martyrs, CS 20156, F-38042 Grenoble Cedex 9, France*

[4]*Consiglio Nazionale delle Ricerche, Istituto Officina dei Materiali c/o Institut Laue-Langevin, 71 avenue des Martyrs, CS 20156, F-38042 Grenoble Cedex 9, France*

(Received 29 October 2016; published 23 January 2017)

We show that by exploiting multi-Lorentzian fits of the self-dynamic structure factor at various wave vectors it is possible to carefully perform the $Q \to 0$ extrapolation required to determine the spectrum $Z(\omega)$ of the velocity autocorrelation function of a liquid. The smooth Q dependence of the fit parameters makes their extrapolation to $Q = 0$ a simple procedure from which $Z(\omega)$ becomes computable, with the great advantage of solving the problems related to resolution broadening of either experimental or simulated self-spectra. Determination of a single-particle property like the spectrum of the velocity autocorrelation function turns out to be crucial to understanding the whole dynamics of the liquid. In fact, we demonstrate a clear link between the collective mode frequencies and the shape of the frequency distribution $Z(\omega)$. In the specific case considered in this work, i.e., liquid Au, analysis of $Z(\omega)$ revealed the presence, along with propagating sound waves, of lower frequency modes that were not observed before by means of dynamic structure factor measurements. By exploiting *ab initio* simulations for this liquid metal we could also calculate the transverse current-current correlation spectra and clearly identify the transverse nature of the above mentioned less energetic modes. Evidence of propagating transverse excitations has actually been reported in various works in the recent literature. However, in some cases, like the present one, these modes are difficult to detect in density fluctuation spectra. We show here that the analysis of the single-particle dynamics is able to unveil their presence in a very effective way. The properties here shown to characterize $Z(\omega)$, and the information in it contained therefore allow us to identify it with the density of states (DoS) of the liquid. We demonstrate that only nonhydrodynamic modes contribute to the DoS, thus establishing its purely microscopic origin. Finally, as a by-product of this work, we provide our estimate of the self-diffusion coefficient of liquid gold just above melting.

DOI: 10.1103/PhysRevE.95.012141

I. INTRODUCTION

In the last two decades the interpretation of the dynamical properties of simple and complex fluids has undergone an enormous evolution. The paradigmatic case of water and its puzzling dynamics, as revealed from the first spectroscopic and simulation studies comprehensively summarized in Refs. [1,2], has opened the way to general progress in the field and to a more complex picture about the longitudinal and shear collective modes that can be sustained (and detected) in a real liquid. In particular, a paper about water by Sampoli *et al.* [3] was the first to suggest a richer dynamical behavior of liquids, with transverse and longitudinal vibrational components both present and visible in nominally "pure" longitudinal and transverse current correlation spectra. At that time, and even afterwards, the explanation about the apparently peculiar dynamics of water and of other molecular liquids, with respect to other simpler fluids, was often attempted in terms of the most striking difference between water (or water-like liquids) and noble gas or metallic liquids: hydrogen bonding. For instance, the onset of shear wave propagation was initially associated with the bending of three hydrogen-bonded molecules [3–6], and, more recently, it has been related to the existence of a structural relaxation process driven by the forming and breaking of hydrogen bonds [2]. Thus, hydrogen bonding has usually been invoked to account for the experimental observation of a second low-frequency branch in the dispersion curve of water, which appears as the counterpart of a transverse acoustic excitation in a solid, as well as the high-frequency one being typically (and more confidently) assigned to the propagation of a longitudinal acoustic wave in the medium.

The presence of shear waves in simpler liquids, such as liquid Rb [7] and Na and Ar [8,9], had, however, been hypothesized and supported by molecular dynamics simulations of the velocity autocorrelation function (VAF) well before the direct experimental observation of transverse modes from the total dynamic structure factor $S(Q,\omega)$ of water. Actually, experimental access to the VAF frequency spectrum $Z(\omega)$ is in principle possible through neutron incoherent scattering, which is the only spectroscopic technique able to probe the single-particle dynamic structure factor $S_{\rm self}(Q,\omega)$ at the inverse picosecond ω scale. $S_{\rm self}(Q,\omega)$, in the limit of vanishing wave vector $Q \to 0$, is related to the VAF spectrum [10], which has a few times been referred to as the density of states (DoS) [11,12], generalizing a solid-state concept. However, the physical implications of such an identification, exploited in Ref. [12], were not, to our knowledge, pursued further in liquid dynamics studies. It was very recently shown that the way in which collective modes produce their signature on the $Z(\omega)$ of a Lennard-Jones (LJ) fluid indeed permits interpretation of the VAF spectrum as the global DoS of a liquid [13], with the difference from the solid case that it has a nonzero $\omega = 0$ value due to diffusion. With this in mind, and identifying $Z(\omega)$ with the liquid DoS, it is clear why the analysis of this quantity becomes of invaluable help as well in investigations of the

collective dynamics of condensed systems. However, $Z(\omega)$ cannot be reliably determined from $S_{\rm self}(Q,\omega)$ data affected by resolution effects, as recognized in the experimental papers devoted to such an attempt [11,14,16]. In particular, the $Q \to 0$ extrapolation, to be performed at fixed ω, of spectra measured at finite Q, becomes critical in the presence of a resolution broadening that grows in importance as Q is decreased [since the width of $S_{\rm self}(Q,\omega)$ spectra reduces as Q^2]. On the other hand, it is very difficult to perform a deconvolution. Finally, another problem discussed in Refs. [11,14–16] concerned the appropriate functional form of the Q dependence to be used for extrapolation. So, on the one hand, accurate extraction of the VAF spectrum from $S_{\rm self}(Q,\omega)$ determinations turned out not to be a simple task at all. On the other hand, the interest in this function was, at that time, focused on the detection of the long-time tail phenomenon (see Ref. [17] for a recent review), so that the great potential of $Z(\omega)$ determination for more general dynamical considerations remained partly obscure and was not pursued further.

In more recent years, discussion about the transverse dynamics of liquids strongly came into the foreground due to experiments revealing the existence of a second low-frequency branch in the dispersion curve not only of associated liquids [18], but also of several liquid metals, as probed by x rays [19–23] and neutron [24] spectroscopy. In one case [24], the nature of the modes was more confidently assigned by comparison of the dispersion curve of the liquid with the DoS of the system in the solid phase, which indeed showed maxima related to transverse and longitudinal modes in agreement with the features and frequencies of the two branches measured in the molten metal. The existence and detectability of shear modes in these systems have sometimes been attributed to anisotropic interactions giving rise to particular structural properties, like the presence of dimers and instantaneous cage formation [19,22]. It is also believed that the specific structural features of a metal in the crystalline phase, i.e., the more or less pronounced anisotropy of the structure in which a system tends to crystallize, might provide an indication about the greater or lower visibility of a richer dynamical behavior in the $S(Q,\omega)$ of liquids. In this respect, liquid gold (fcc in the solid phase) might be expected to show a simpler dynamics, at the level of $S(Q,\omega)$, than liquid zinc (hcp in the solid phase and with an anomalous c/a ratio) [24]. However, this was not the case of liquid sodium, which, despite the rather simple crystal structure (bcc in the solid phase), was claimed to show shear modes directly in the x-ray spectra [20,21].

Indeed, our study of the dynamics of liquid gold [25] at a temperature just above melting ($T = 1373$ K) at room pressure, performed through the combined analysis of scattering data collected at the neutron Brillouin spectrometer BRISP (Institut Laue Langevin, Grenoble) [26] and *ab initio* simulation results for the dynamic structure factor $S(Q,\omega)$, shows a rather familiar behavior, with a single acoustic mode perfectly accounting for the inelastic part of the spectrum, and with a dispersion curve clearly longitudinal in nature. The viscoelastic analysis (see Ref. [27] for a review) of the simulated $S(Q,\omega)$ provided excellent fits, and later attempts to include a second possible inelastic mode in the fit function gave a worse description of the spectra. In addition, a deeper statistical Bayesian analysis of the experimental data set recently confirmed that the presence of a second inelastic mode is not justified on a statistical basis within the accuracy of the available $S(Q,\omega)$ data [28]. These findings are, however, not conclusive about the absence of transverse modes in liquid gold because several effects, for instance, a too low intensity, might hinder their direct detection. Access to the DoS of the liquid would therefore be extremely useful to better probe the vibrational dynamics in cases like the one of liquid gold and could become a powerful method to establish whether the presence of shear modes is a more general feature of liquids.

Here we show that this is indeed possible by taking advantage of the progresses made both in the theory of correlation functions of many-body systems [29–31] and in computing power, the latter allowing, at present, *ab initio* simulations of reasonable accuracy. It is important to stress, however, that the case of gold is taken here merely as an example, albeit a significant one, and that the method we propose in no way requires the use of simulated data, as done in this work to test our procedure, but opens instead a main route towards a successful experimental determination of the DoS of a liquid.

II. THEORETICAL CONSIDERATIONS

As shown in recent papers [29–31], the functionality of time correlation functions is established on a solid theoretical basis. The theory states that any time correlation function is exactly represented by an infinite series of exponentials of generally complex argument. In formulas, given a normalized autocorrelation function $b(t)$ of a classical system, its representation at $t \geqslant 0$ is

$$b(t) = \frac{\langle B(0)B(t)\rangle}{\langle B^2\rangle} = \sum_{k=1}^{\infty} I_k e^{z_k t}, \tag{1}$$

where I_k and z_k are amplitude and complex frequency, respectively, of the kth mode. When I_k and z_k are complex quantities, both the corresponding mode and its conjugate ($I_{k+1} = I_k^*$, $z_{k+1} = z_k^*$) are present and, summed together, describe an exponentially damped oscillation. When I_k and z_k are real the mode represents instead a pure exponential decay. For all modes ${\rm Re}z_k$ is negative, thus the damping is to be identified with $-{\rm Re}z_k$.

The spectrum of $b(t)$, defined as its Fourier transform (FT) $b(\omega) = \frac{1}{2\pi}\int_{-\infty}^{\infty} b(t)e^{-i\omega t}\,dt$, is given by

$$b(\omega) = \sum_{k=1}^{\infty} b_k(\omega) = \sum_{k=1}^{\infty} \frac{1}{\pi}{\rm Re}\frac{I_k}{i\omega - z_k}, \tag{2}$$

where $b_k(\omega)$ is a generalized Lorentzian line. If I_k and z_k are real, then $b_k(\omega)$ is a true Lorentzian:

$$b_k(\omega) = I_k \frac{1}{\pi}\frac{(-z_k)}{\omega^2 + z_k^2}. \tag{3}$$

If I_k and z_k are complex, then the corresponding mode (k) and its conjugate ($k+1$) sum together to give a pair of distorted

inelastic Lorentzians:

$$b_k(\omega)+b_{k+1}(\omega) = \frac{1}{\pi}\mathrm{Re}\left[\frac{I_k}{i\omega-z_k}+\frac{I_k^*}{i\omega-z_k^*}\right] = \frac{I_k'}{\pi}\left[\frac{-z_k'+I_k''/I_k'(\omega-z_k'')}{(\omega-z_k'')^2+(z_k')^2}+\frac{-z_k'-I_k''/I_k'(\omega+z_k'')}{(\omega+z_k'')^2+(z_k')^2}\right], \quad (4)$$

where the prime and double prime are used to indicate the real and imaginary parts of the complex quantities. We have adopted here the following convention: if a mode has $z_k = -|z_k'|+i|z_k''|$, then its amplitude is written as $I_k = I_k'+iI_k''$ where I_k' and I_k'' have no restriction in sign. Correspondingly, $z_k^* = -|z_k'|-i|z_k''|$ and $I_k^* = I_k'-iI_k''$.

Exploiting the relation between the $p-$th time derivative of $b(t)$ in $t=0$ and the pth frequency moment $\langle\omega^p\rangle$ of the spectrum $b(\omega)$, a set of sum rules can be defined as

$$\sum_{k=1}^{\infty} I_k z_k^p = i^p\langle\omega^p\rangle. \quad (5)$$

Since we are presently considering a classical system, for which autocorrelations are even functions of time, all odd frequency moments are known and equal to zero. Moreover, with $b(t)$ normalized to unity at $t=0$, the $p=0$ sum rule is $\sum_{k=1}^{\infty} I_k = 1$.

An extremely simple result, but of great importance for the next determination of the liquid DoS, is the one regarding the correlation function related to the second time derivative of $b(t)$, that is, the correlation

$$c(t) = \frac{\langle\dot{B}(0)\dot{B}(t)\rangle}{\langle B^2\rangle} = -\ddot{b}(t) \quad (6)$$

whose spectrum is $c(\omega)=\omega^2 b(\omega)$.

However, direct differentiation of $b(t)$ gives, for $t\geqslant 0$, and according to Eq. (1)

$$c(t) = \sum_{k=1}^{\infty}\left(-I_k z_k^2\right)e^{z_k t}, \quad (7)$$

so that its spectrum can also be written as

$$c(\omega) = \sum_{k=1}^{\infty}\frac{1}{\pi}\mathrm{Re}\frac{\left(-I_k z_k^2\right)}{i\omega-z_k}. \quad (8)$$

Therefore, from Eqs. (2) and (8), it is seen that

$$c(\omega) = \omega^2\sum_{k=1}^{\infty}\frac{1}{\pi}\mathrm{Re}\frac{I_k}{i\omega-z_k} = \sum_{k=1}^{\infty}\frac{1}{\pi}\mathrm{Re}\frac{\left(-I_k z_k^2\right)}{i\omega-z_k}. \quad (9)$$

Note that the last equality in Eq. (9) is a straightforward algebraic identity, as it can be seen by taking the difference between the two sides of the equation, and writing $\omega^2+z_k^2$ as $(i\omega-z_k)(-i\omega-z_k)$. The first factor cancels out the denominator, leaving $(1/\pi)\mathrm{Re}\sum_{k=1}^{\infty} I_k(-i\omega-z_k)$, which can be written as $(1/\pi)\mathrm{Re}[-i\omega(\sum_{k=1}^{\infty} I_k)-(\sum_{k=1}^{\infty} I_k z_k)]$. The last expression equals zero due to the sum rules of Eq. (5) with $p=0,1$.

Despite its simplicity, such a relation carries the important meaning that the autocorrelation function of a dynamical variable $B(t)$ and that of its derivatives are characterized by the same time decays or complex frequencies and therefore describe essentially the same dynamics. The same generalized Lorentzians describe the spectra $b(\omega)$ and $c(\omega)$, with only different amplitudes, where those of $c(\omega)$ are readily obtained by multiplying the amplitudes of $b(\omega)$ by the negative of the squared "generalized half-width" z_k (either real or complex).

While the multiexponential expansion [Eq. (1)] applies to any correlation function, and the corresponding multi-Lorentzian representation [Eq. (2)] describes the respective spectrum, the result expressed by Eq. (8) is of particular importance in those cases in which two physically meaningful autocorrelation functions are linked by a double time differentiation. A well-known example is the case of the intermediate scattering function $F(Q,t)$ and the longitudinal current autocorrelation $C_L(Q,t)$ [10]. Here, however, we are concerned with the self-intermediate scattering function,

$$F_{\mathrm{self}}(Q,t) = \langle e^{-i\mathbf{Q}\cdot\mathbf{R}(0)}e^{i\mathbf{Q}\cdot\mathbf{R}(t)}\rangle, \quad (10)$$

where $\mathbf{R}(t)$ is the position of any tagged particle, and with the VAF:

$$Z(t) = \langle\mathbf{v}(0)\cdot\mathbf{v}(t)\rangle, \quad (11)$$

where $\mathbf{v}(t)$ is the velocity of one particle at time t, and $\langle ...\rangle$ includes an average over all particles. By performing a double differentiation of Eq. (10) and exploiting the isotropy of a liquid, one obtains the exact result

$$Z(t) = \lim_{Q\to 0}\left[-\frac{3}{Q^2}\ddot{F}_{\mathrm{self}}(Q,t)\right] \quad (12)$$

[see Eq. (1.54) of Ref. [10]], which relates $Z(t)$ to the second time derivative of $F_{\mathrm{self}}(Q,t)$. Correspondingly, Fourier transformation of Eq. (12) provides the link between the spectrum of the VAF and the self-part $S_{\mathrm{self}}(Q,\omega)$ of the dynamic structure factor. In Sec. III we will exploit this result and the direct connection that Eq. (9) therefore establishes between their respective multi-Lorentzian expansions.

The exponential mode expansion method is to be applied by a suitable truncation of the infinite series depending on the extension and accuracy of available data, as discussed in Refs. [13,17]. This was successfully done in the time domain to interpret the dynamical behavior of a Lennard-Jones fluid at various densities and temperatures [13,17]. In all analyzed cases it was shown that a limited number of modes was required to achieve an excellent description of the simulated VAF, with a suitable number of obeyed moment sum rules. Here we show that an identical situation is found in the frequency domain, and by considering the spectrum ($S_{\mathrm{self}}(Q,\omega)$) of a different autocorrelation function ($F_{\mathrm{self}}(Q,t)$).

III. METHODOLOGY AND RESULTS

Being interested here in the determination of the DoS of a liquid starting from self-spectra, we investigated the case of liquid Au, for which ab initio simulations of $S_{\mathrm{self}}(Q,\omega)$ were available to apply the previous concepts. Stored particle configurations also allowed us to directly evaluate the VAF of liquid gold, providing in this way the basis of a consistency

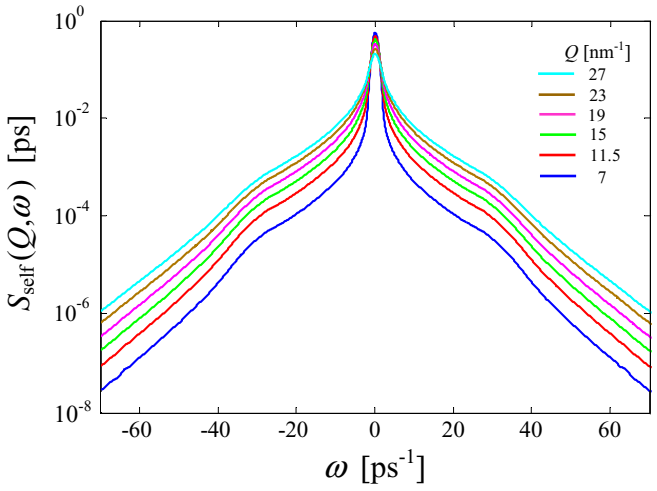

FIG. 1. Self-dynamic structure factor of liquid Au obtained by *ab initio* simulations at the Q values reported in the legend. Spectral intensities at large ω grow monotonically with Q.

check between the two possible routes towards $Z(\omega)$. Details about the simulations are the same as those given in Ref. [25].

Figure 1 shows the gold self-spectra at some example Q values of the simulations. The use of a semilogarithmic scale immediately highlights the presence of at least one shoulder located at $\omega \simeq 30$ ps^{-1}, which is also found at all investigated Q values.

Despite this rather surprising result for the shape of $S_{\rm self}(Q,\omega)$, usually not investigated in such a wide ω range, it will be clear in the following that these shoulders are genuine features of the spectra which are approximately positioned at the same frequency where maxima in the longitudinal dispersion curve take place [see Fig. 7 in Ref. [25]]. This preliminary observation will find an explanation in the next discussion of the DoS; however, it is useful to anticipate that the spectral features of $S_{\rm self}(Q,\omega)$ at large ω are strictly linked to those of the DoS.

In order to illustrate the relation between the DoS and $S_{\rm self}(Q,\omega)$, it is useful to introduce $Z_{\rm E}(Q,\omega)$, defined as

$$Z_{\rm E}(Q,\omega) = \frac{3\omega^2}{Q^2} S_{\rm self}(Q,\omega), \tag{13}$$

the $Q \to 0$ limit of which is the sought DoS according to the Fourier transform of Eq. (12), also known as Egelstaff formula (indicated by the subscript E) [32]:

$$Z_{\rm E}(\omega) = \lim_{Q\to 0} Z_{\rm E}(Q,\omega) = \lim_{Q\to 0} \frac{3\omega^2}{Q^2} S_{\rm self}(Q,\omega). \tag{14}$$

However, the above definition of $Z_E(\omega)$ hides a discontinuity in $\omega = 0$, since different results are obtained for $Z_{\rm E}(\omega = 0)$ depending on the order used to perform the $Q \to 0$ and $\omega \to 0$ limits in Eq. (14) [14]. In particular, it is only by performing the $Q \to 0$ limit before the $\omega \to 0$ one that Eq. (14) provides the correct zero-frequency value $Z(0) = 3D_s/\pi$, with D_s the self-diffusion coefficient. This value is obtained straightforwardly from the Green-Kubo relation [10] $D_s = (1/3)\int_0^\infty dt\, Z(t)$ and considering that $\int_0^\infty dt Z(t) = \pi Z(\omega = 0)$. By recalling that in the hydrodynamic $Q \to 0$ regime $S_{\rm self}(Q,\omega)$ reduces to the one-Lorentzian spectrum predicted by Fick's law of simple diffusion:

$$S_{\rm self}(Q \to 0,\omega) = \frac{1}{\pi} \frac{D_s Q^2}{\omega^2 + D_s^2 Q^4}, \tag{15}$$

it is seen that by performing the limits in the reverse order one obtains the wrong result $Z_{\rm E}(\omega = 0) = 0$.

Morkel and Gronemeyer [14] have shown that the pathological behavior of $Z_{\rm E}(\omega)$ in $\omega = 0$ can be corrected, and the quoted discontinuity removed, by replacing $Z_{\rm E}(Q,\omega)$ with

$$Z(Q,\omega) = \frac{3}{Q^2} S_{\rm self}(Q,\omega)\left(\omega^2 + D_s^2 Q^4\right), \tag{16}$$

which is continuous also in the origin ($Q = 0$ and $\omega = 0$) and provides $Z(\omega)$ as

$$Z(\omega) = \lim_{Q\to 0} Z(Q,\omega). \tag{17}$$

Note that the above redefinition makes it correspond to the VAF spectrum as well. In fact, Eq. (16) descends from the FT of

$$Z(Q,t) = -\frac{3}{Q^2} \ddot{F}_{\rm self}(Q,t) + 3D_s^2 Q^2 F_{\rm self}(Q,t), \tag{18}$$

where in the $Q \to 0$ limit the second term vanishes. Combination of Eqs. (16) and (17) and analysis of the $S_{\rm self}(Q,\omega)$ spectra thus allows to determine the DoS as described in the next subsections.

A. Q behavior of the spectral components of $S_{\rm self}(Q,\omega)$

We used the multi-Lorentzian expansion [Eq. (2)] of $S_{\rm self}(Q,\omega)$,

$$S_{\rm self}(Q,\omega) = \sum_{k=1}^{\infty} \frac{1}{\pi} {\rm Re} \frac{I_k(Q)}{i\omega - z_k(Q)}, \tag{19}$$

in order to find, through a fitting procedure, the amplitudes $I_k(Q)$ and complex frequencies $z_k(Q)$ of the modes contributing to the spectra. The convolution of the fitted model with the resolution function (which is known from the simulation method or from the instrumental setup in the case of experimental data) is a very effective way to get rid of any broadening and to obtain results free of resolution effects. An excellent representation of the Au self-spectra was actually obtained by considering six modes: two real modes (labeled as R1 and R2) and four complex modes (indicated as C1 pair and C2 pair), the sum of which was forced to obey the zeroth, first, third, and fifth frequency moment sum rules. These constraints ensure finite even moments of $S_{\rm self}(Q,\omega)$ up to the sixth one, with the resulting second moment checked *a posteriori* to perfectly agree with the theoretical value $k_{\rm B}TQ^2/M$ [10], with $k_{\rm B}$ the Boltzmann constant, T the temperature, and M the atomic mass of gold.

Figure 2 shows the very good performance of the fitted model at two Q values (the second close to Q_p, the position of the main maximum in the static structure factor $S(Q)$). The various components of the global fit function are also plotted to demonstrate the impossibility to reproduce the shape of the self-spectrum with real modes only.

In order to construct $Z(\omega)$ via Eqs. (16) and (17), an analysis of the Q dependence of the various parameters

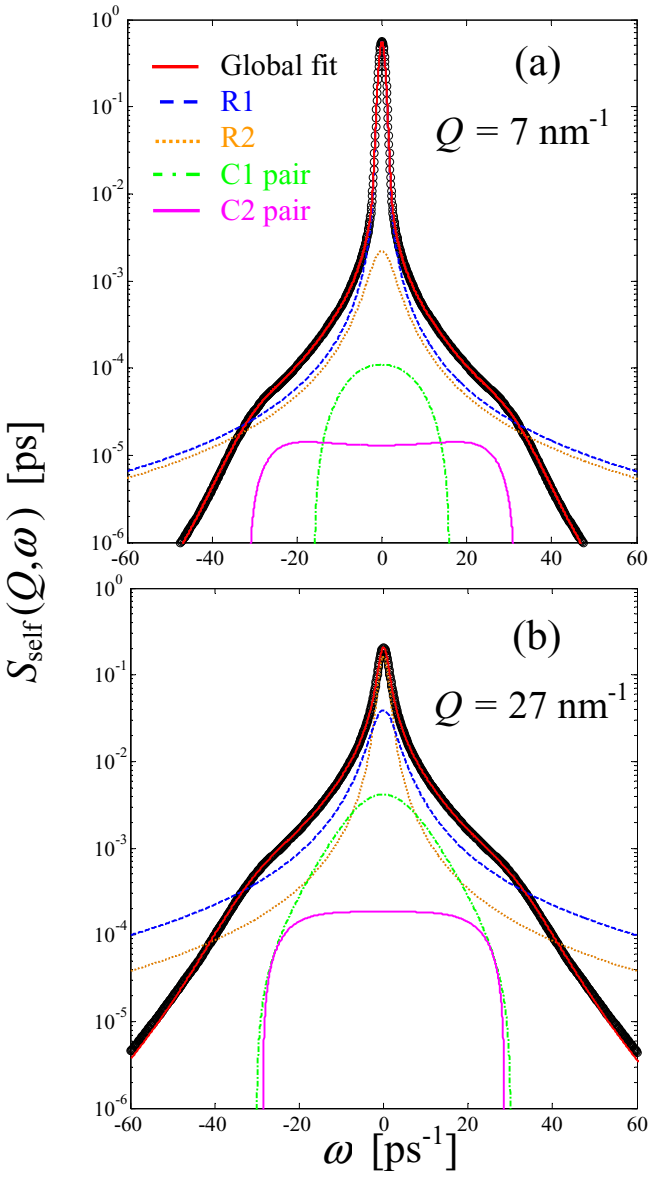

FIG. 2. Self-dynamic structure factor of liquid Au (black circles) at two Q values. The real (dashed blue and dotted orange curves) and complex (solid magenta and dash-dotted green curves) components that give rise to the overall fit curve (red solid curve) are shown along with the simulation data on a semilogarithmic scale. Note that the high-frequency negative wings of the complex pairs cannot appear in the plot.

and a final $Q \to 0$ extrapolation of all of them is required. As Fig. 3 shows, the real and complex eigenfrequencies $z_k(Q)$ and amplitudes $I_k(Q)$ have all very smooth trends that enable a reliable $Q \to 0$ extrapolation by means of polynomials. However, before commenting on an appropriate form for such polynomials, several useful observations are worth anticipating by looking at Fig. 3. In particular, in compliance with the exact hydrodynamic limit, only one mode (R1) is seen from Fig. 3(d) to survive in $S_{self}(Q,\omega)$ as $Q \to 0$, since the amplitudes $I_k(Q)$ of all other modes in Figs. 3(d)–3(f) vanish. Consistently, also the damping $-z_{R1}$ can be recognized at glance to follow the parabolic behavior typical of Fick's simple diffusion, which we find to hold up to the rather high value $Q \simeq 18$ nm^{-1}. Thus, in Fig. 2 R1 can be confidently identified with the pure Lorentzian line predicted by Fick's law.

The other real component (R2), necessary, together with R1, to properly describe the central peak of $S_{self}(Q,\omega)$, displays a nonhydrodynamic behavior witnessed by the almost constant width and by an amplitude that grows with Q to the detriment of the R1 one. It is useful to compare the decay time constant $\tau_{R2} = -1/z_{R2}$ with the Enskog mean collision time τ_E of liquid gold at the number density of melting $\rho = 53.03$ nm^{-3}:

$$\tau_E = \frac{1}{4\rho\sigma^2 g(\sigma)}\sqrt{\frac{M}{\pi k_B T}}, \tag{20}$$

with σ the hard spheres (HS) diameter for liquid gold at melting [33] and $g(\sigma)$ the radial distribution function at contact, taken from the Carnahan-Starling HS equation of state as [34]

$$g(\sigma) = \frac{1 - \pi\rho\sigma^3/12}{(1 - \pi\rho\sigma^3/6)^3}. \tag{21}$$

The result for τ_E turns out to be 0.03 ps, that is approximately 10 times smaller than τ_{R2}. This classifies R2 as a rather slow relaxation process that involves quite a number of collisions, but which is, even so, much faster than the hydrodynamic mode R1, for which $\tau_{R1} = -1/z_{R1} \approx 2$ ps at our highest Q.

The complex contribution C2 is seen to account for the previously commented inelastic feature in $S_{self}(Q,\omega)$ (see Fig. 1), with a frequency in very close agreement with the maximum of the observed dispersion [25] of purely longitudinal propagating sound waves. A similar identification was recently fully justified by a multiexponential analysis of the VAF and its spectra for a LJ high-density fluid [13]. This means that self-correlation functions clearly carry the fingerprints of the underlying collective dynamics, and that these are reflected by the need of including at least one complex mode in the model if a proper description of self-spectra is to be obtained. However, the physical origin of the other complex component (C1) and of the nonhydrodynamic real mode (R2) will be clarified after the next determination of $Z(\omega)$ (see Sec. IV).

The self-intermediate scattering function $F_{self}(Q,t)$ of classical systems is known [35] to be a function of Q^2, and Fourier transformation to $S_{self}(Q,\omega)$ does not alter this property. This suggests that the low-Q dependence of $I_k(Q)$ and $z_k(Q)$ is properly described by Q^2 polynomials of the general form $a + bQ^2 + cQ^4 + \cdots$ (where the first term may be missing for some of the parameters) and that the $Q \to 0$ behavior can be determined by fitting such polynomials. In the used fit range (7 nm$^{-1} < Q < 20$ nm^{-1}) it turns out to be sufficient to limit oneself to Q^4 terms for all parameters $I_k(Q)$ and $z_k(Q)$. In more detail, and recalling that R1 can be identified with Fick's mode, it is seen from Fig. 3 that the Q behavior of the parameters is very well accounted for by the following expansions, without the need to include odd powers of Q:

$$\begin{aligned} I_{R1}(Q) &= 1 + O(Q^2) \\ z_{R1}(Q) &= -D_s Q^2 + O(Q^4) \end{aligned} \tag{22}$$

for the first real mode R1 ($k = 1$), and

$$\begin{aligned} I_k(Q) &= p_k Q^2 + O(Q^4) \\ z_k(Q) &= z_k(0) + O(Q^2) \end{aligned} \tag{23}$$

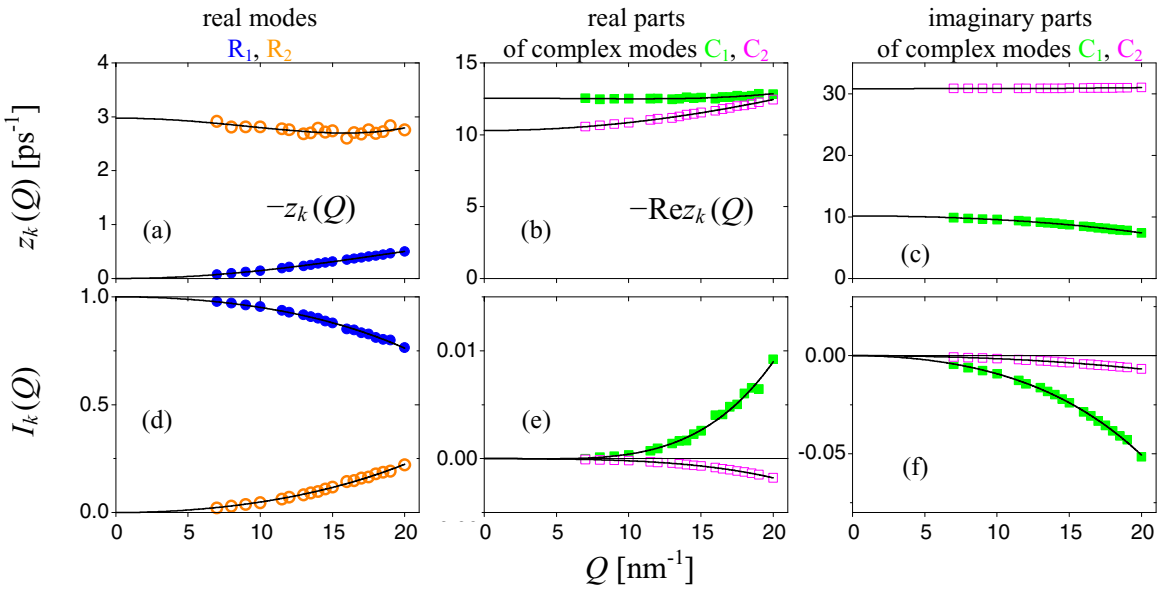

FIG. 3. Q dependence of the parameters z_k (top frames) and I_k (bottom frames), fitted to $S_{\mathrm{self}}(Q,\omega)$ data. In each row, the left panel refers to the two real exponential modes (labeled R1 and R2, and displayed as dots and open circles, respectively), the center and right panels display the real and imaginary parts of the parameters of the two pairs of complex modes (labeled C1 and C2, and displayed as filled and empty squares, respectively). In all frames, the colors are those indicated in the top labels. Black solid lines represent the best fitting polynomials in powers of Q^2 up to the Q^4 term. In (a) and (b) the absolute values of the negative quantities z_k and $\mathrm{Re}z_k$ are plotted. For each complex pair we chose to plot the amplitude (with its own sign) of the mode in the pair having $\mathrm{Im}z_k > 0$.

for all the other modes ($k \geqslant 2$), with the parameters p_k independent of Q.

We stress that the Q^2 coefficient in the fit function of $z_{\mathrm{R1}}(Q)$, i.e., $-D_s$, was left as a free parameter. In fact, no experimental determination of D_s for liquid gold appears to be available, and calculated or simulated estimates often disagree, with a range of variability between 0.6 and 3.5 $\times 10^{-3}$ nm^2 ps^{-1} [36–38]. Our fit provides $D_s = 1.5\times10^{-3}$ nm^2 ps^{-1}, in good agreement with the calculation of Ref. [36] and with one of the values of Ref. [38].

B. Q behavior of the mode expansion of $Z(Q,\omega)$ and determination of $Z(\omega)$

The previous analysis of $S_{\mathrm{self}}(Q,\omega)$ allows us, through the general relations of Eqs. (2), (9), (16), and (19), to derive $Z(Q,\omega)$ as

$$Z(Q,\omega) = \sum_{k=1}^{\infty} \frac{1}{\pi} \mathrm{Re} \frac{A_k(Q)}{i\omega - z_k(Q)}, \tag{24}$$

with amplitudes of the modes given by

$$A_k(Q) = -\frac{3}{Q^2} z_k^2(Q) I_k(Q) + 3D_s^2 Q^2 I_k(Q). \tag{25}$$

Using Eqs. (17) and (24), the DoS is therefore obtained as

$$Z(\omega) = \lim_{Q\to 0} Z(Q,\omega) = \sum_{k=1}^{\infty} \frac{1}{\pi} \mathrm{Re} \frac{A_k(Q\to 0)}{i\omega - z_k(Q\to 0)}, \tag{26}$$

which requires the determination of the $Q \to 0$ limit of the various $A_k(Q)$. Before discussing the extrapolation, important insight is provided by the analysis of Fig. 4 where we report,

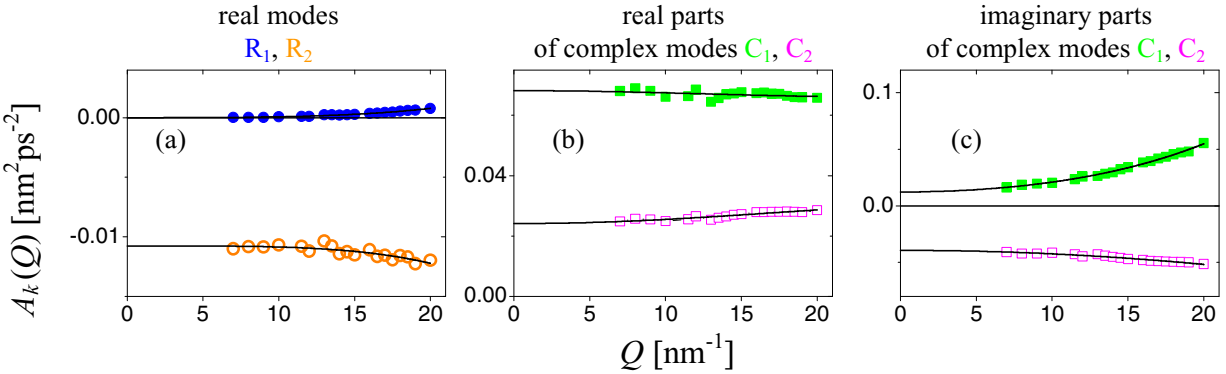

FIG. 4. As in Fig. 3 for the amplitudes A_k of the modes contributing to $Z(Q,\omega)$.

for all real and complex modes, the amplitudes of Eq. (25) as a function of Q. From Fig. 4 it is immediately evident that one component [R1, panel (a)] has a vanishing amplitude at low Q. This actually means that the Fick's mode R1, so important in the description of $S_{\rm self}(Q,\omega)$ at small Q and which gives, in addition, the only surviving Lorentzian in $S_{\rm self}(Q,\omega)$ as $Q \to 0$, actually *does not* contribute to the DoS [Eq. (26)] at any frequency. Thus, the presence of mass diffusion, witnessed by one of the modes of $S_{\rm self}(Q,\omega)$, is accounted for in $Z(\omega)$ by *all modes but* R1. It is straightforward to show that it is the combination of the other three modes that provides the correct nonzero $Z(0)$ starting value of the DoS. To this aim we insert Eq. (26) into the Green-Kubo relation that yields D_s and perform the integration, obtaining

$$D = \frac{1}{3}\sum_k \lim_{Q\to 0}\left(-\frac{A_k}{z_k}\right), \tag{27}$$

and using Eqs. (22) and (23) it is easy to find that the R1 mode gives a null contribution to the sum. The other terms together provide the value $\sum_{k\geqslant 2} p_k z_k(0)$, which can be evaluated using the $p = 1$ sum rule, as follows:

$$0 = \sum_k I_k(Q) z_k(Q) = -D_s Q^2 + \sum_{k\geqslant 2} p_k z_k(0) Q^2 + O(Q^4)$$

$$= Q^2\left[-D_s + \sum_{k\geqslant 2} p_k z_k(0)\right] + O(Q^4), \tag{28}$$

which shows that

$$\sum_{k\geqslant 2} p_k z_k(0) = D_s. \tag{29}$$

Therefore, the contribution of the various modes of $S_{\rm self}(Q,\omega)$ to the diffusion coefficient satisfies a null sum rule, which in the $Q \to 0$ limit entrusts the value of the Green-Kubo integral to the remaining microscopic (nonhydrodynamic) modes R2, C1, and C2, which together yield the expected macroscopic transport coefficient related to the $\omega = 0$ value of the DoS.

We now turn to the final evaluation of Eq. (26). Given the quality of the Q fits to the various $I_k(Q)$ and $z_k(Q)$ of Fig. 3 and recalling Eq. (25), $A_k(Q)$ is also of course well described by polynomials of the form $a + bQ^2 + cQ^4 + \cdots$, as shown in Fig. 4. In order to reach a better numerical accuracy we preferred to fit the polynomials to the $A_k(Q)$ themselves to obtain their limit values $A_k(Q \to 0)$, rather than deriving them from Eq. (25) using the previously determined $I_k(Q \to 0)$ and $z_k(Q \to 0)$. In this way we determined the amplitudes of the various terms of Eq. (26), and we finally calculated the DoS reported in Fig. 5, along with its components.

In order to better validate such an experimentally applicable method to access the $Z(\omega)$ of a liquid via possible incoherent neutron-scattering experiments, we also directly computed the liquid gold VAF and the transverse current correlation spectra $C_{\rm T}(Q,\omega)$ [39] from the available *ab initio* simulations. Figure 6 shows the comparison of the just described DoS determination with the one obtained by direct Fourier transformation of the simulated VAF. It is evident from Fig. 6 that agreement is remarkable, suggesting that the multi-Lorentzian fit to $S_{\rm self}(Q,\omega)$ and subsequent extrapolation of the related

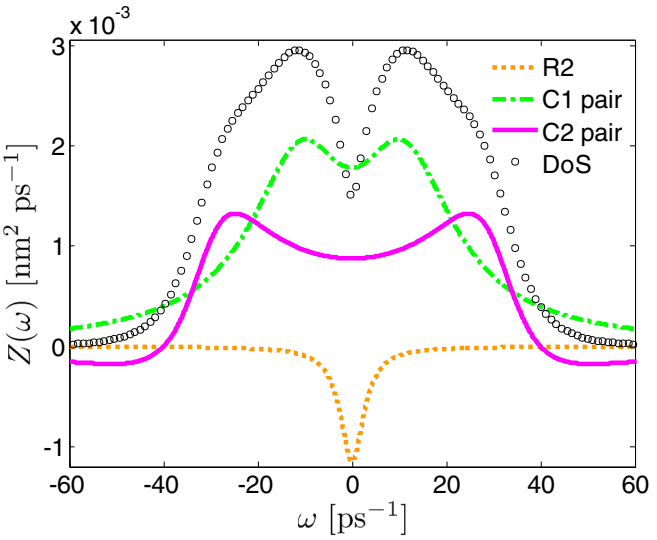

FIG. 5. Density of states $Z(\omega)$ of liquid Au as obtained from the analysis of $S_{\rm self}(Q,\omega)$ spectra with the method described in Sec. III. The DoS (black circles) is shown along with its Lorentzian components specified in the legend.

parameters provides indeed the true limit $Z(\omega)$ curve. This strong consistency between very different ways of determining the DoS (the second possible only if simulation data are available) has a great significance *per se* and represents an important result of the proposed method. Obviously the two routes also provide the same D_s value.

We note from Figs. 4(a) and 5 that the real mode R2 has a negative amplitude $A_{\rm R2}$, in agreement with Eq. (25) where the first term is negative and the second becomes negligible for small Q values. This can be understood on physical grounds by recalling the behaviors of the amplitude $I_{\rm R2}$ and damping $-z_{\rm R2}$ in Figs. 3(a) and 3(d), which induce us to relate this mode to a trapping mechanism that tends to confine the particle,

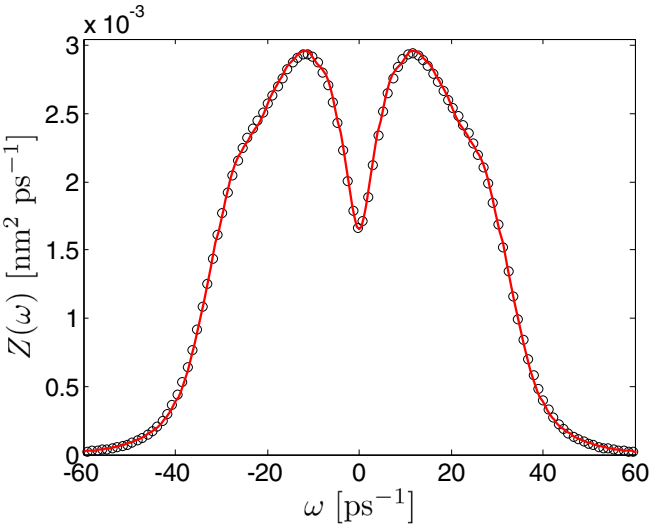

FIG. 6. $Z(\omega)$ as obtained with the procedure leading to Fig. 5 (black circles) and by direct time FT of the simulation-derived VAF (red solid curve).

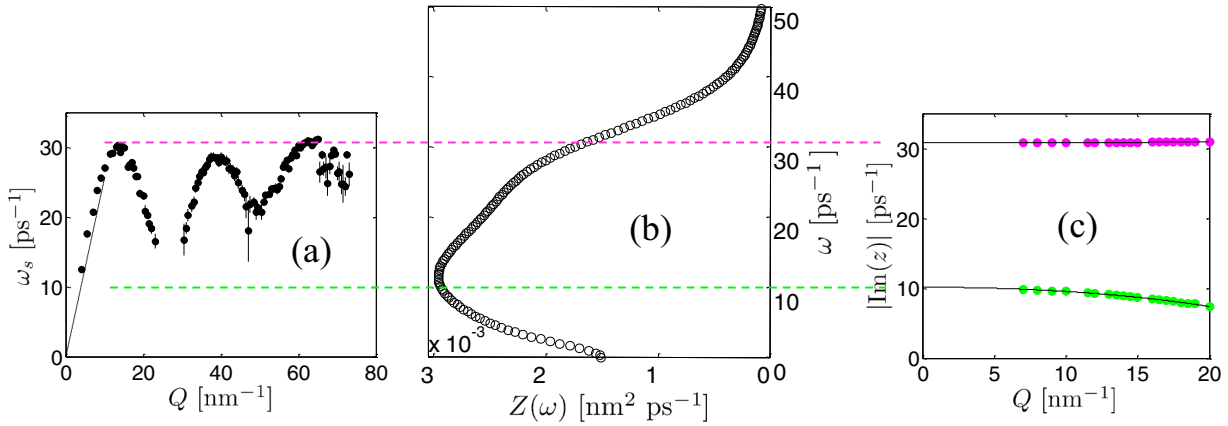

FIG. 7. Dispersion curve of longitudinal modes of liquid gold as obtained in Ref. [25], compared with the shape of $Z(\omega)$. The maxima in the dispersion curve occur at frequencies in agreement with the shoulder in the DoS (the dashed pink line is a guide to the eye). Conversely $S(Q,\omega)$ determinations miss the second branch accounting for the maximum in $Z(\omega)$. The last right panel is the same as that of Fig. 3(c) and shows how the frequency of the C2 modes of $Z(\omega)$ agrees with the features of the longitudinal dispersion curve.

hindering diffusion in high-density liquids. In this picture, $\tau_{R2} = -1/z_{R2}$, which is almost constant with Q, assumes the meaning of a residence time, after which the particle is able to diffuse again under the global effect of shear and acoustic waves traveling in the medium. Actually, such a sort of diffusion-hindering phenomena can show up only as negative Lorentzians in the spectrum of the VAF, not only because of the mathematical relation of Eq. (25), but also because confinement physically corresponds to mechanisms that reduce the diffusion coefficient and the low-frequency part of $Z(\omega)$.

IV. $Z(\omega)$ AND COLLECTIVE DYNAMICS

These overall results indicate that, albeit its fully single-particle character, $Z(\omega)$ is a very fruitful quantity also for the understanding of the collective dynamics at a microscopic level. As mentioned, the C2 component can be ascribed to the collective longitudinal excitations present in the liquid. As regards the C1 pair, we are induced to identify it as due to *transverse* acoustic modes contributing to the overall cooperative motions that the single-particle behavior cannot avoid to mirror. Such a preliminary identification of C1 with the collective transverse contribution to the DoS is also in agreement with the typical behavior in the solid state case, where dispersion curves of transverse phonons involve typically lower frequencies and have a flatter Q dependence than longitudinal ones [giving rise to a visible peak in $Z(\omega)$ at low frequency].

The direct connection between the shape of $Z(\omega)$ and the presence of longitudinal and transverse modes in a dense liquid is clarified in Figs. 7 and 8. Figure 7 shows how maxima in the dispersion curve, derived by determinations of the $S(Q,\omega)$ of liquid Au [25], find their evidence in the $Z(\omega)$ considered in the present work. We recall that the analysis of neutron and simulation data of $S(Q,\omega)$ for this specific liquid did not justify (even on a statistical basis [28]) the inclusion of more than one (longitudinal) excitation in the model fit function. However, as Fig. 7 shows, deep investigation of the overall dynamics requires more than considering $S(Q,\omega)$ only.

In the case of liquid gold, transverse low-frequency modes, though likely weak in intensity and undetectable from $S(Q,\omega)$ data, emerge neatly at the level of the VAF spectrum and of $C_T(Q,\omega)$. The peak around 10 ps^{-1} in $Z(\omega)$ is indeed consistent with the behavior of the transverse current correlation spectra shown in Fig. 8. The maximum developing at nonzero frequency above $Q \simeq 6$ nm^{-1} in $C_T(Q,\omega)$ indicates the onset of transverse modes propagation in liquid gold at our thermodynamic conditions. The frequency of the maximum increases with Q, but, after about 17 nm^{-1}, it stabilizes around 10 ps^{-1}. This means that, correspondingly, the transverse dispersion curve tends to flatten above this Q value, producing a maximum in $Z(\omega)$. Finally, as observed in other cases, the first of which represented to our knowledge by the paper of Sampoli *et al.* [3], the $C_T(Q,\omega)$ of liquid Au also shows evidence of a longitudinal contribution (an increasing bump around 25–30 ps^{-1}).

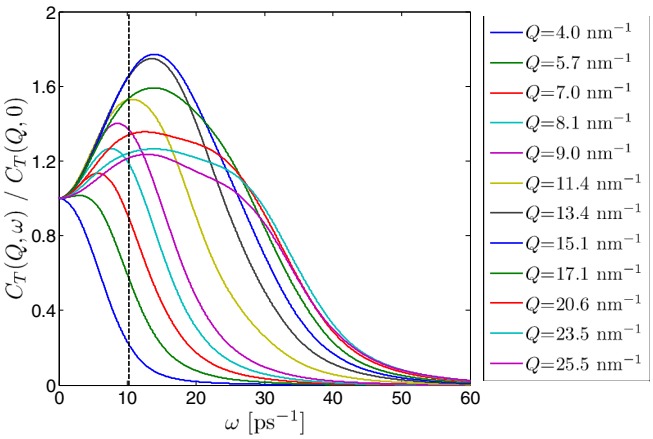

FIG. 8. Transverse current correlation spectra calculated from the *ab initio* simulations and normalized to their $\omega = 0$ values. Several Q values are displayed in order to follow the onset of visible shear modes propagation above 6 nm^{-1}. The shapeless curves correspond to the lower Q values, while those developing a shoulder around 25 ps^{-1} correspond to the highest Q. The vertical dashed black line gives the frequency position of the main maximum in $Z(\omega)$, either from Fig. 5 or from Fig. 6.

Some comments are also worth making about another, implicit but significant, result of this work. In Refs. [13,17] the multi-exponential analysis was applied directly in the time domain to the simulated VAF of a LJ fluid in various thermodynamical states. For one of them, that nearest to the triple point (at least in density), the mode expansion was found to include three complex pairs and two real modes. One of the complex modes, of negligible intensity, represents a very fast oscillation of $Z(t)$ which, in the present case, is not detected in $S_{\rm self}(Q,\omega)$ because it would contribute to the farthest spectral wings. The other two complex modes correspond precisely, and with the same physical origin, to those denoted here as C1 and C2. A very slowly decaying real exponential, found in the LJ case to be the remnant of the long-time tail in the VAF, does not appear in the gold case, in agreement with the absence of a tiny peak at $\omega \simeq 0$ in the spectrum of the liquid gold VAF (Fig. 5), which is instead the typical spectral fingerprint of the presence of a very slow process [see, for instance, Fig. 5(d) of Ref. [13]]. This indicates that in dense liquids much closer to the triple point (both in density and temperature), as in the present case, such a very slow real mode becomes undetectable due to a too short recurrence time of the simulations, a well-known problem related to the simulation box length (see, for instance, Ref. [17] and references there reported), which limits the time range of reliability of the calculations. The only remaining real mode found in the mentioned LJ-fluid high-density state corresponds to R2 here, and in both the LJ and liquid gold case this contributes with a negative central Lorentzian to $Z(\omega)$. As explained, some modes of the LJ fluid cannot be observed in the gold case; however, no modes different from those here labeled as R2, C1, and C2 are found. Therefore, considering the different thermodynamic states, the self-dynamics undergoes the same mode expansion, and with the same physical meaning of each mode, for systems as different as a model LJ fluid and a real liquid metal. In other words identical representations and identifications hold for the two mentioned cases.

V. CONCLUSIONS

We have clearly shown the following in this work:

(1) A reliable access to the $Z(\omega)$ of a liquid is possible. The method here proposed proves extremely accurate and provides resolution-free results. It is a merit of the multi-exponential expansion of time correlation functions, applied also in this work, to render the $Q \to 0$ extrapolation of the data easy, with a consequently very precise determination of the limit curve $Z(\omega)$ on an absolute scale. In addition, when the directly simulated VAF spectrum is compared to our determination of $Z(\omega)$, the two spectra are found to coincide perfectly.

(2) Single-particle correlation functions and their spectra carry precious information about the collective dynamics of liquids and reflect faithfully the whole atomic motion. The VAF and its spectrum are therefore indispensable quantities to analyze if the whole dynamics is to be understood and disclosed in its various contributions. In particular, this work confirms the findings of Ref. [13] and reinforces the conceptual identification of $Z(\omega)$ with the density of states of a liquid. It is also clearly shown here that the macroscopic diffusion coefficient related to $Z(0)$ comes from the composition of nonhydrodynamic modes, and that the Fick's mode in $S_{\rm self}(Q,\omega)$ does not determine any feature of the DoS of a liquid. Although $Z(\omega)$ is obtained in the $Q \to 0$ limit, this means that the DoS is built up by microscopic modes. This is consistent with the results of the LJ case, where no Fick's mode was found from fits performed directly on the VAF, and the diffusion coefficient was given by the time integral of other modes.

(3) Transverse propagating modes appear in liquid Au as in other systems, but only the analysis of the DoS could clearly confirm, also for this liquid, what is starting to be accepted as a general property of dense fluids.

(4) Models of the self-dynamics based on the multiexponential expansion or on its time FT lead to the same real and complex mode decomposition for dense liquids of disparate nature, with a total correspondence in the modes' physical meaning.

This last point suggests that the exponential expansion method might provide an innovative tool for interpreting other physical phenomena in the microscopic dynamics of disordered systems, among which, for instance, the long debated issue about the well-known anomaly in the DoS of many glasses, namely, the Boson peak.

ACKNOWLEDGMENT

We thank Daniele Colognesi for extremely clarifying discussions.

[1] G. Ruocco and F. Sette, J. Phys.: Condens. Matter **11**, R259 (1999).
[2] A. Cunsolo, Adv. Condens. Matter Phys. **2015**, 137435 (2015), and references therein.
[3] M. Sampoli, G. Ruocco, and F. Sette, Phys. Rev. Lett. **79**, 1678 (1997).
[4] S. Krishnamurthy, R. Bansil, and J. Wiafe-Akenten, J. Chem. Phys. **79**, 5863 (1983).
[5] G. E. Walrafen, J. Phys. Chem. **94**, 2237 (1990).
[6] F. Formisano and S. De Panfilis, Phys. Rev. Lett. **115**, 149801 (2015), and references therein.
[7] T. Gaskell and S. Miller, J. Phys. C **11**, 3749 (1978).
[8] T. Gaskell and S. Miller, J. Phys. C **11**, 4839 (1978).
[9] T. Gaskell and S. Miller, J. Phys. C **12**, 2705 (1979).
[10] U. Balucani and M. Zoppi, *Dynamics of the Liquid State* (Clarendon Press, Oxford, 1994).
[11] C. Morkel, C. Gronemeyer, W. Gläser, and J. Bosse, Phys. Rev. Lett. **58**, 1873 (1987).
[12] K. Toukan, M. A. Ricci, S.-H. Chen, C.-K. Loong, D. L. Price, and J. Teixeira, Phys. Rev. A **37**, 2580 (1988).
[13] S. Bellissima, M. Neumann, E. Guarini, U. Bafile, and F. Barocchi, Phys. Rev. E **95**, 012108 (2017).

[14] C. Morkel and C. Gronemeyer, Z. Phys. B **72**, 433 (1988).
[15] W. Montfrooij and I. de Schepper, Phys. Rev. A **39**, 2731 (1989).
[16] P. Verkerk, J. Westerweel, U. Bafile, L. A. de Graaf, W. Montfrooij, and I. M. de Schepper, Phys. Rev. A **40**, 2860 (1989).
[17] S. Bellissima, M. Neumann, E. Guarini, U. Bafile, and F. Barocchi, Phys. Rev. E **92**, 042166 (2015).
[18] S. Bellissima, S. De Panfilis, U. Bafile, A. Cunsolo, M. A. González, E. Guarini, and F. Formisano, Sci. Rep. **6**, 39533 (2016).
[19] S. Hosokawa, M. Inui, Y. Kajihara, K. Matsuda, T. Ichitsubo, W.-C. Pilgrim, H. Sinn, L. E. González, D. J. González, S. Tsutsui, and A. Q. R. Baron, Phys. Rev. Lett. **102**, 105502 (2009).
[20] V. M. Giordano and G. Monaco, Proc. Natl. Acad. Sci. USA **107**, 21985 (2010).
[21] V. M. Giordano and G. Monaco, Phys. Rev. B **84**, 052201 (2011).
[22] S. Hosokawa, S. Munejiri, M. Inui, Y. Kajihara, W.-C. Pilgrim, Y. Ohmasa, S. Tsutsui, A. Q. R. Baron, F. Shimojo, and K. Hoshino, J. Phys.: Condens. Matter **25**, 112101 (2013).
[23] S. Hosokawa, M. Inui, Y. Kajihara, S. Tsutsui, and A. Q. R. Baron, J. Phys.: Condens. Matter **27**, 194104 (2015).
[24] M. Zanatta, F. Sacchetti, E. Guarini, A. Orecchini, A. Paciaroni, L. Sani, and C. Petrillo, Phys. Rev. Lett. **114**, 187801 (2015).
[25] E. Guarini, U. Bafile, F. Barocchi, A. De Francesco, E. Farhi, F. Formisano, A. Laloni, A. Orecchini, A. Polidori, M. Puglini, and F. Sacchetti, Phys. Rev. B **88**, 104201 (2013).
[26] F. Formisano, A. De Francesco, E. Guarini, A. Laloni, A. Orecchini, C. Petrillo, W.-C. Pilgrim, D. Russo, and F. Sacchetti, J. Phys. Soc. Jpn. **82**, SA028 (2013).
[27] U. Bafile, E. Guarini, and F. Barocchi, Phys. Rev. E **73**, 061203 (2006).
[28] A. De Francesco, E. Guarini, U. Bafile, F. Formisano, and L. Scaccia, Phys. Rev. E **94**, 023305 (2016).
[29] F. Barocchi, U. Bafile, and M. Sampoli, Phys. Rev. E **85**, 022102 (2012).
[30] F. Barocchi and U. Bafile, Phys. Rev. E **87**, 062133 (2013).
[31] F. Barocchi, E. Guarini, and U. Bafile, Phys. Rev. E **90**, 032106 (2014).
[32] P. A. Egelstaff, *An Introduction to the Liquid State* (Academic Press, New York, 1967).
[33] P. Protopapas, H. C. Andersen, and N. A. D. Parlee, J. Chem. Phys. **59**, 15 (1973).
[34] J. P. Hansen and I. R. McDonald, *Theory of Simple Liquids* (Academic Press, London, 1986).
[35] B. R. A. Nijboer and A. Rahman, Physica **32**, 415 (1966).
[36] R. N. Joarder and R. V. Gopala Rao, Phys. Status Solidi B **109**, 137 (1982).
[37] A. Bogicevic, L. B. Hansen, and B. I. Lundqvist, Phys. Rev. E **55**, 5535 (1997).
[38] S. Ryu, C. R. Weinberger, M. I. Baskes, and W. Cai, Modell. Simul. Mater. Sci. Eng. **17**, 075008 (2009).
[39] For the definition of the current correlation functions we follow Ref. [10] and write $C_{\mathrm{T}}(Q,t) = 1/(2N)\langle \mathbf{j}_{\mathrm{T}}^{*}(\mathbf{Q},0)\cdot \mathbf{j}_{\mathrm{T}}(\mathbf{Q},t)\rangle$, where $\mathbf{j}_{\mathrm{T}}(\mathbf{Q},t) = \mathbf{j}(\mathbf{Q},t) - \mathbf{j}_{\mathrm{L}}(\mathbf{Q},t)$, $\mathbf{j}_{\mathrm{L}}(\mathbf{Q},t) = (\mathbf{j}(\mathbf{Q},t)\cdot \mathbf{Q})\mathbf{Q}/Q^2$ and finally $\mathbf{j}(\mathbf{Q},t) = \sum_{\alpha} \mathbf{v}_{\alpha}(t)\exp[i\mathbf{Q}\cdot\mathbf{R}_{\alpha}(t)]$ where $\mathbf{R}_{\alpha}(t)$ and $\mathbf{v}_{\alpha}(t)$ are position and velocity of the αth particle.